ANTIOXIDANTS & REDOX SIGNALING
Volume 12, Number 5, 2010

DOI: 10.1089/ars.2009.2862

Hypoxia Increases ROS Signaling and Cytosolic Ca^{2+} in Pulmonary Artery Smooth Muscle Cells of Mouse Lungs Slices

Jennifer R. Desireddi,[1] Kathryn N. Farrow,[1] Jeremy D. Marks,[2]
Gregory B. Waypa,[1] and Paul T. Schumacker[1]

Abstract

Precapillary arteries constrict during alveolar hypoxia in a response known as hypoxic pulmonary vasoconstriction (HPV). The mechanism by which pulmonary arterial smooth muscle cells (PASMCs) detect a decrease in Po_2 and trigger contraction is not fully understood. Previous studies in cultured PASMCs show that hypoxia induces an increase in reactive oxygen species (ROS) production, but these results may not reflect responses of PASMCs in their native tissue environment. We therefore assessed hypoxia-induced changes in cytosolic ROS in PASMCs of precision-cut mouse lung slices expressing the redox-sensitive protein, RoGFP. Superfusion of lung slices with hypoxic media (1.5% O_2) resulted in a significant oxidation of RoGFP from normoxic baseline that was attenuated by overexpression of cytosolic catalase. Hypoxic superfusion also increased $[Ca^{2+}]_i$ above normoxic baseline; this response was significantly attenuated by cytosolic catalase overexpression or by the administration of EUK134, a synthetic SOD-catalase mimetic. The hypoxia-induced increase in $[Ca^{2+}]_i$ was abolished in the absence of extracellular Ca^{2+}, indicating that ROS signals trigger entry of extracellular calcium. Collectively, these results indicate that an increase in cytosolic ROS signaling is required for the increase in $[Ca^{2+}]_i$ in PASMCs in precision-cut mouse lung slices during the acute HPV response. *Antioxid. Redox Signal.* 12, 595—602.

Introduction

Microvascular pulmonary arteries constrict during alveolar hypoxia in a response known as hypoxic pulmonary vasoconstriction (HPV). Acute HPV directs blood flow toward well-ventilated areas of the lung, thereby optimizing gas exchange. HPV responses have been measured in whole lung, isolated PA vessels, and isolated pulmonary artery smooth muscle cells (PASMCs), indicating that the O_2-sensing machinery is intrinsic to PASMCs. The mechanism by which PASMCs detect a decrease in Po_2 and transduce this into a cellular signaling mechanism resulting in a contraction is not fully understood. Two opposing HPV models have emerged, linking mitochondria-dependent reactive oxygen species (ROS) signaling to O_2 sensing during hypoxia. One model proposes that ROS signaling decreases during hypoxia (1, 23). Conversely, we have proposed that hypoxia induces an increase in ROS production (21). The resulting increase in oxidative signaling then potentially triggers Ca^{2+} release from the sarcoplasmic reticulum (3–9) and entry of extracellular calcium through voltage-dependent calcium channels, as well as capacitative calcium entry (CCE) through store-operated calcium channels (SOCCs), resulting in contraction (16, 17). In support of this, overexpression of catalase or glutathione peroxidase-1 (GP_x1), and diverse pharmacologic antioxidants, blocks the HPV response (8, 18, 20). In addition, exogenous H_2O_2 mimics HPV in intact isolated lungs and PASMCs (18, 20).

In prior studies, we detected the hypoxia-induced increase in ROS signaling as measured by using a redox-sensitive FRET sensor (HSP-FRET), whereas the corresponding increase in $[Ca^{2+}]_i$ was measured by using FURA-2 in the same PASMCs (19). However, smooth muscle cells can undergo changes in phenotype during culture, so the relevance of these findings to the intact lung must be established. Moreover, interactions between PASMCs and endothelium or other cells can influence and possibly enhance the HPV response (9). Paddenberg and colleagues (13) directly demonstrated HPV

[1]Department of Pediatrics, Division of Neonatology, Northwestern University, Feinberg School of Medicine, Chicago, Illinois.
[2]Department of Pediatrics, University of Chicago, Chicago, Illinois.

in intra-acinar mouse pulmonary vessels in mouse precision-cut lung slices (PCLSs) by using media gassed with 1% O_2. They also showed vasoconstriction in the microvasculature of PCLSs in response to the thromboxane analogue U46619. They observed that hypoxia-induced vasoconstriction in PCLSs was blocked by the superoxide scavenger nitroblue tetrazolium, suggesting the involvement of ROS production in HPV (13). To examine the role of ROS signaling in the hypoxic response of PASMCs in their normal cell–cell environment, we measured ROS and Ca^{2+} signaling in PASMCs of arterial segments in mouse PCLSs during acute hypoxia.

Materials and Methods

Mouse precision-cut lung slices

Animal protocols were reviewed and approved by the IACUC. Adult mice were anesthetized with ketamine (40 mg/kg) and xylazine (3 mg/kg). The trachea was cannulated with a 24-gauge angiocatheter. The heart and lungs were removed *en bloc* by using aseptic technique. The pulmonary artery was cannulated with a 1.9-Fr catheter and infused with 0.05% agarose containing Cell Tracker Red (Invitrogen, Carlsbad, CA) to label endothelial cells of the vessels. The lungs were then expanded with 1.5 ml of 0.1% low-melting-temperature agarose *via* the trachea cannula. The lungs and heart were placed in cold PBS + 25 m*M* HEPES to gel the agarose. By using a Leica Microsystems (Setzlar, Germany) VT 1000S tissue slicer, 200-μm-thick lung slices were obtained and maintained in serum-free M199 media.

ROS-signaling measurements

To measure changes in ROS signaling during hypoxia in lung slices, RoGFP, a redox-sensitive protein sensor, was used (5, 7, 14). The RoGFP protein was generated from a mammalian expression vector (pEGFP-N1) by using a Stratagene Quick-Change Kit (Agilent Technologies, La Jolla, CA), and then subcloned into an adenoviral shuttle vector to permit generation of a recombinant adenovirus to facilitate efficient expression of the probe in primary cells. This redox-sensitive protein exhibits reciprocal emission when excited at 400 and 488 nm, when reduced and oxidized (5), allowing it to function as a thiol redox sensor in the cytosol where it is expressed. Moreover, these changes are dynamic and reversible, allowing it to be calibrated at the end of an experiment by administration of a reducing agent [dithiothreitol (1 m*M*)] and oxidizing agent [*tert*-butyl hydroperoxide (1 m*M*)] (7). Adenoviral RoGFP (1×10^7 pfu/μl) was administered to the lung slices and allowed to incubate in serum-free media at 37°C for 3 h. Then, complete media (M199 + 10% serum) was added to the slices, and they were incubated further for a total of 48 h to allow expression of the protein.

Cytosolic calcium measurements

Hypoxia-induced changes in $[Ca^{2+}]_i$ were measured by using FURA-2 (Invitrogen, Carlsbad, CA). FURA-2 is excited at 340 nm and 380 nm, whereas emission is measured at 595 nm. The ratio of the emissions at those wavelengths is directly related to the concentration of cytosolic calcium. Lung slices were loaded with FURA-2AM at 37°C (5 μM) for 1 h before imaging. The lung slices were then incubated for an additional 15 min in medium without FURA-2AM to allow esterases to cleave the diacetate moiety completely (20). Although FURA-2AM was taken up by most cells within the lung slice, $[Ca^{2+}]_i$ measurements were restricted to regions localized to pulmonary arteries identified by Cell Tracker Red. In selected studies, hypoxia-induced changes in $[Ca^{2+}]_i$ were measured by using FURA-2 in the absence of extracellular Ca^{2+} to determine the contribution of calcium entry in the response to hypoxia.

Calcium responses in PCLS were evident in slices incubated for 24 h, but became difficult to detect after 48 h in culture. Therefore, all $[Ca^{2+}]_i$ measurements were made within 24 h of slicing.

Antioxidants

In selected studies, lung slices were infected with adenoviral catalase (1×10^6 pfu/μl), an antioxidant enzyme expressed in peroxisomes in the cytosol. The lung slices were then incubated at 37°C for 24 or 48 h to allow expression of catalase. In similar studies, lung slices were incubated with FURA-2AM or EUK134 (20 μM), a synthetic SOD-catalase mimetic (Cayman Chemical Company, Ann Arbor, MI) for 1 h before fluorescence imaging. EUK134 concentrations were maintained in the perfusate throughout the experiments.

Fluorescence imaging

Lung slices were studied in a flow-through chamber between glass coverslips under controlled O_2 conditions on an inverted fluorescence microscope. Images were collected every 20 s. Normoxia was maintained by superfusing the slices with a balanced salt solution (BSS: NaCl (177 m*M*), KCl (4.0 m*M*), $NaHCO_3$ (18 m*M*), $MgSO_4$, (0.76 m*M*), NaH_2PO_4 (1 m*M*), $CaCl_2$ (1.21 m*M*), and glucose (5.6 m*M*) that was bubbled with 21% O_2, 5% CO_2, and 74% N_2 gas mixture. Hypoxia was induced by bubbling the perfusate with a 1.5% O_2, 5% CO_2, and 94% N_2 gas mixture. Angiotensin II (5 μM) was used to demonstrate precapillary contraction and PCLS viability under normoxic conditions (data not shown). Video capture was used to demonstrate precapillary vasoconstriction under hypoxic conditions. Image J software was used to measure the luminal cross-sectional area during normoxia and subsequent hypoxia. In studies using RoGFP, the oxidizing agent *tert*-butyl hydroperoxide (1 m*M*) and the reducing agent dithiothreitol (1 m*M*) (Sigma-Aldrich, St. Louis, MO) were used to calibrate the RoGFP protein sensor at the end of each experiment. To assess hypoxia-induced $[Ca^{2+}]_i$ signaling responses in cells perfused with salt solutions, ET-1 (endothelin, 10 n*M*, American Peptide, Sunnyvale, CA) was added to the perfusate to prime the lung cells, as described previously (18). ET-1 concentrations (10 ng/ml) were maintained throughout the experiment. Imaging data acquisition and analysis was accomplished by using MetaMorph/MetaFluor software (Molecular Devices, Downingtown, PA).

Immunostaining and lung-slice confocal imaging

To determine whether the RoGFP protein was being expressed in the PASMCs of the lung slice, 200-μm lung slices were fixed in 4% formaldehyde for 20 min and then washed 3 times in PBS for 5 min. Each lung slice was then placed in 0.1% Triton X100 for 20 min and then washed 3 times in

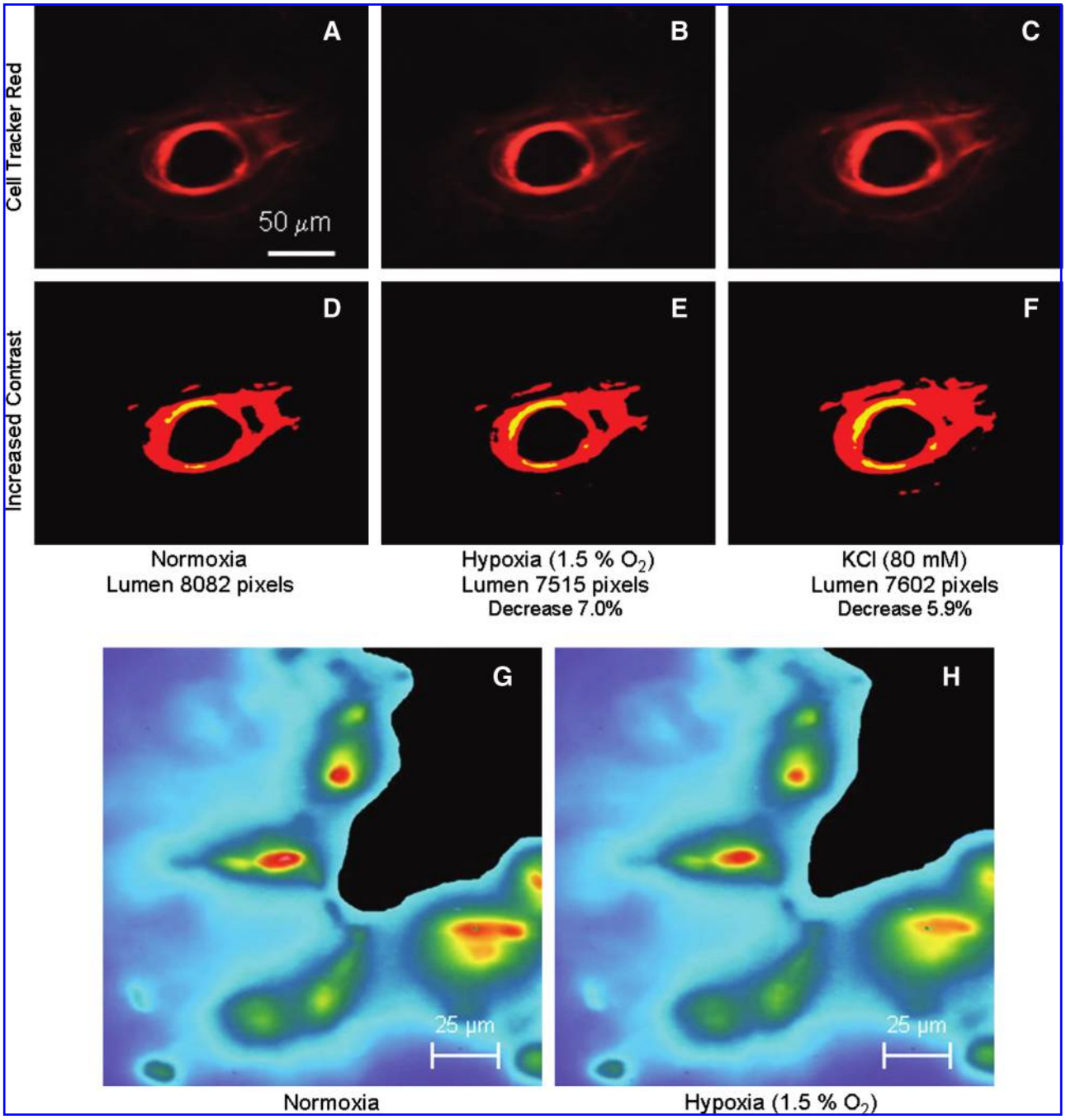

FIG. 1. (A–F) Fluorescence images of a pulmonary artery within a lung slice (200 μm thick), labeled with Cell Tracker Red dye *via* vascular perfusion, under normoxic (A, D), hypoxic (B, E), and high-potassium (C, F) conditions. Hypoxia and high potassium each elicited vasoconstriction, resulting in a decrease of luminal cross-sectional area. (**G**, **H**) False color ratiometric images of a pulmonary artery within a lung slice expressing RoGFP in vascular cells. Hypoxia (1.5% O_2) elicited a decrease in vessel lumen area and a shift in cellular redox toward a more reduced state (less red, more blue) (**H**). (For interpretation of the references to color in this figure legend, the reader is referred to the web version of this article at www.liebertonline.com/ars).

PBS for 5 min. Finally, the lung slices were placed in 5% BSA for 1 h. The slices were then labeled with a smooth muscle cell–specific primary antibody, anti-desmin antibody (rabbit; Sigma, St. Louis, MO; 1:50 dilution), overnight at 37°C. The lung slices were washed with PBS and labeled with a secondary antibody, anti-rabbit 633 (Alexa Fluor 633; Molecular Probes/InVitrogen, Carlsbad, CA; 1:300 dilution) for 3 h. The slices were mounted and fixed to a slide with a coverslip. Confocal images were obtained by using a Zeiss LSM 510 META laser scanning confocal microscope with a 40× oil immersion lens and the Zeiss LSM imaging software (Carl Zeiss MicroImaging, Thornwood, NY). Emission was measured at 525 nm for RoGFP, 543 nm for Cell Tracker Red, and 633 nm for the smooth muscle cell immunostaining. This process was

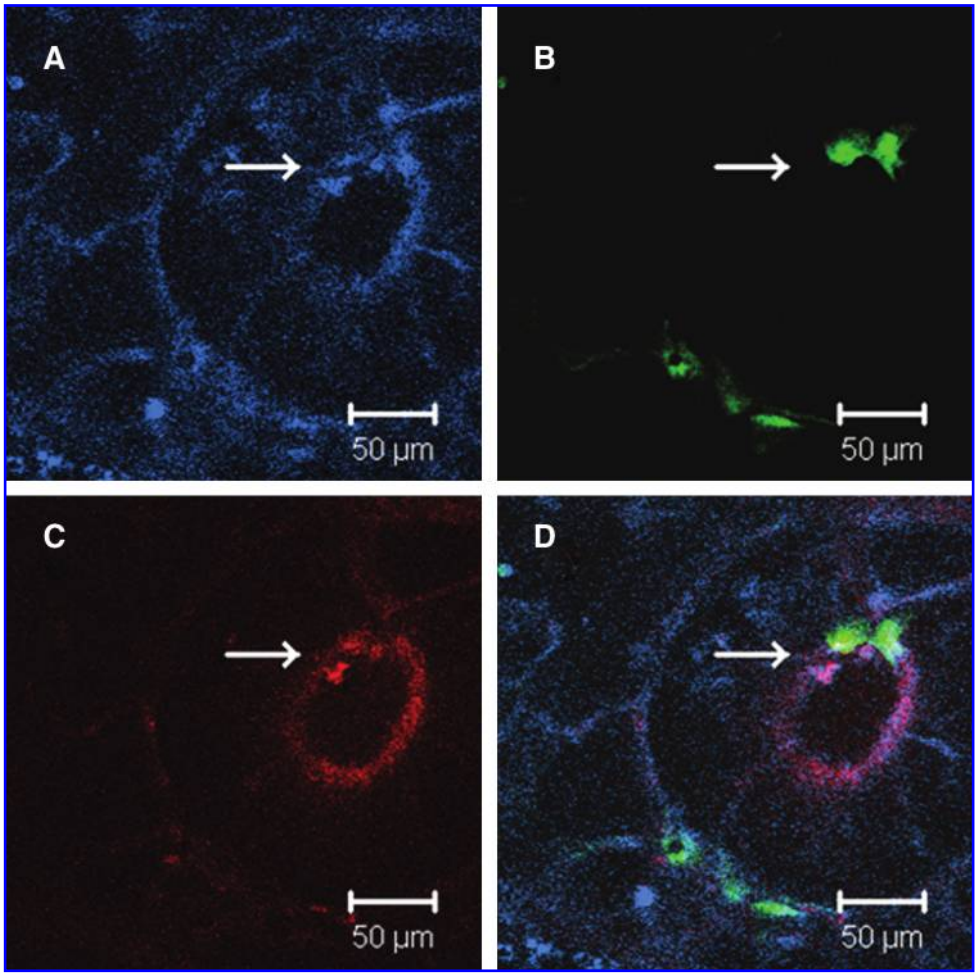

FIG. 2. Confocal image of a mouse lung slice (200 μm thick). PASMCs were labeled by using anti-desmin antibody (A, blue). The lung slice was transduced in culture with a recombinant adenovirus expressing RoGFP targeted to the cytosol (**B**). Endothelial cells were labeled with Cell Tracker Red before slicing (**C**). The green RoGFP protein (**B**) colocalized with the anti-desmin antibody (**A**) in PASMCs in the wall of the pulmonary artery (**D**). (For interpretation of the references to color in this figure legend, the reader is referred to the web version of this article at www.liebertonline.com/ars).

repeated by using anti-catalase primary antibody (rabbit; Abcam, Cambridge, MA; 1:50 dilution) in 200-μm-thick lung slices that had been treated with adenoviral catalase to evaluate catalase expression in comparison to control slices.

Statistics

Data are expressed as mean ± standard error of the mean. Each n value represents a PASMC region, with two to six PASMC regions analyzed per lung slice. A minimum of four lung slices were used per experiment. An ANOVA for repeated measures was used to identify significant differences between groups. *Post hoc* testing was performed by using the Newman–Keuls test. To control for differences in the hypoxic responses, experimental studies and control experiments were always performed on the same day. Statistical significance was set at $p < 0.05$ (15).

Results

With video capture, precapillary arteries within a normoxic PCLS demonstrated vasoconstriction in response to angiotensin II, thus indicating viability of the preparation (data not shown). Figure 1 represents a set of images of an intraparenchymal pulmonary artery, visualized by using Cell Tracker Red fluorescence, under normoxic conditions (A, D), during hypoxia (B, E), and in response to KCl administration (C, F). With Image J software, the lumen of the vessel was traced in the images, and the area was determined to be 8,082 pixels during normoxia, 7,515 during hypoxia, and 7,602 during KCl perfusion. In another lung slice, representative ratiometric images of RoGFP were obtained under normoxic and hypoxic conditions (Fig. 1G and H). The vessel lumen area was 39,432 pixels during normoxia and 34,292 pixels during hypoxia, reflecting a 13% decrease. In concert with the contraction, an oxidative shift in RoGFP redox status in the smooth muscle cells was observed during hypoxia. Thus, pulmonary arteries of PCLS maintain their constrictive properties.

RoGFP expression within PASMCs of lung slices was assessed by using immunostaining techniques and imaged by laser scanning confocal microscopy. PASMCs (blue) were identified by staining with anti-desmin antibody, which localized to a region outside the pulmonary artery lumen (Fig. 2A). RoGFP protein expression (green) was evident in cells

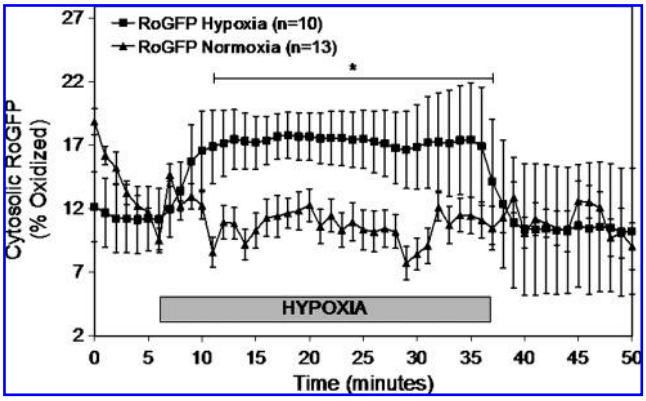

FIG. 3. Hypoxia significantly increases ROS signaling in PASMCs of mouse lung slices when compared with normoxic perfusion. The redox-sensitive protein sensor RoGFP was expressed in the cytosol. Superfusion of the lung slices with hypoxic media resulted in an increase in oxidation of the RoGFP protein. Values are expressed as mean ± SEM. $^*p \leq 0.05$.

localized to the region outside the pulmonary artery lumen as well (Fig. 2B). The pulmonary vasculature was identified by using Cell Tracker Red, which had been administered *via* the pulmonary artery before slicing (Fig. 2C). When these images were merged, the desmin-positive and RoGFP-expressing signals colocalized within the same cells lining the pulmonary arterial lumen (Fig. 2D). These findings indicate that the RoGFP protein was effectively expressed in PASMCs within the pulmonary artery wall in the mouse lung slices.

We previously reported that ROS signaling in cultured PASMCs progressively increases during hypoxia (19). However, PASMCs may undergo phenotypic changes while in culture. Therefore, we measured changes in ROS signaling in PASMCs of arterial segments in 200-μm lung slices under controlled O_2 conditions by using RoGFP. Superfusion of the lung slices with hypoxic media (30 min) caused rapid and significant oxidation of the RoGFP sensor (17.7 ± 4.5% oxidized) when compared with superfusion with normoxic media (11.2 ± 2.5% oxidized) (Fig. 3). This indicates that the O_2 sensor and signaling mechanism of PASMCs for intact lung slices behaves similarly, although much more rapidly, compared with cultured PASMCs (not shown). Oxidation of the RoGFP protein was sustained throughout the hypoxia challenge. Removal of the hypoxic stimulus was associated with a rapid restoration of baseline redox status, indicating that the RoGFP protein was rereduced by reductases in the cells, most likely glutaredoxin (6).

To determine whether the RoGFP sensor was responding to an ROS signal, we overexpressed cytosolic catalase to enhance the scavenging of H_2O_2 in the cells. When compared with the low level of endogenous catalase expression in the vascular wall (Fig. 4A, blue), catalase overexpression produced a significant increase (Fig. 4E; blue). Transduction with adenovirus to express RoGFP yielded the expected fluorescence in the vessel wall (Fig. 4B), which was unaffected in slices overexpressing catalase (Fig. 4F; green). Cell Tracker Red was administered *via* the pulmonary artery before slicing to facilitate identification of pulmonary vessels during confocal imaging (Fig. 4C and G; red). The overlay images (Fig. 4D and H) demonstrate colocalization of the RoGFP protein and catalase.

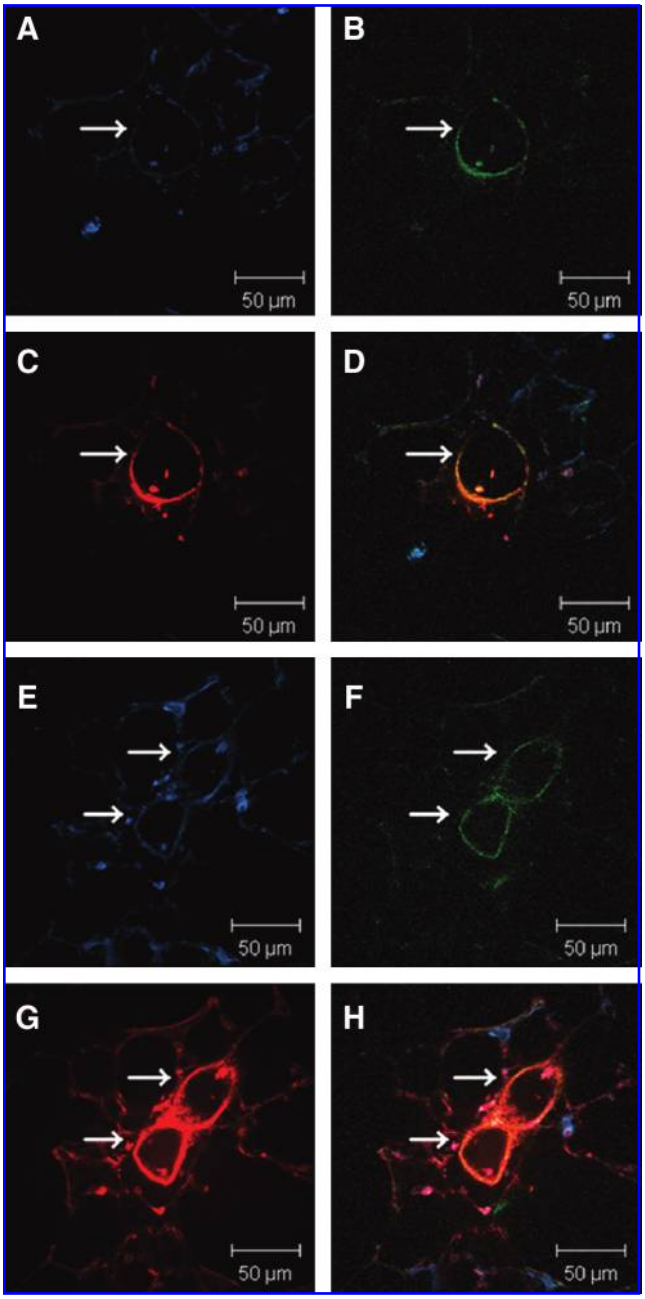

FIG. 4. Confocal images of two mouse lung slices (200 μm thick) showing endogenous levels of catalase (A) compared with a lung slice transduced with adenoviral catalase (E). Overexpression of catalase did not affect the adenoviral expression of cytosolic RoGFP (**F** compared with **B**). Endothelial cells were labeled with Cell Tracker Red before slicing (**C**, **G**). Overlay images (**D**, **H**) illustrate the colocalization of RoGFP and catalase in cells surrounding the pulmonary artery lumen. (For interpretation of the references to color in this figure legend, the reader is referred to the web version of this article at www.liebertonline.com/ars).

Under baseline normoxic conditions, reducing conditions predominate in the cytosol of vascular cells, as indicated by the redox status of RoGFP, which exhibited only 10 to 15% oxidation (Fig. 5). During acute hypoxia (1.5% O_2), a small but significant increase in oxidation developed, with RoGFP

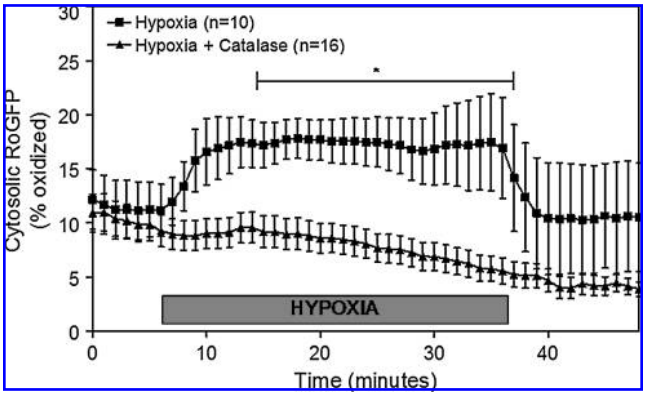

FIG. 5. Lung slices were transduced with a recombinant adenovirus expressing RoGFP in the cytosol. Cells expressing RoGFP in the wall of the pulmonary artery were imaged. Superfusion of the lung slices with hypoxic media for 30 min elicited an increase in oxidation of the RoGFP sensor. This response was significantly attenuated by overexpression of cytosolic catalase. Values are expressed as mean ± SEM. $^*p \leq 0.05$.

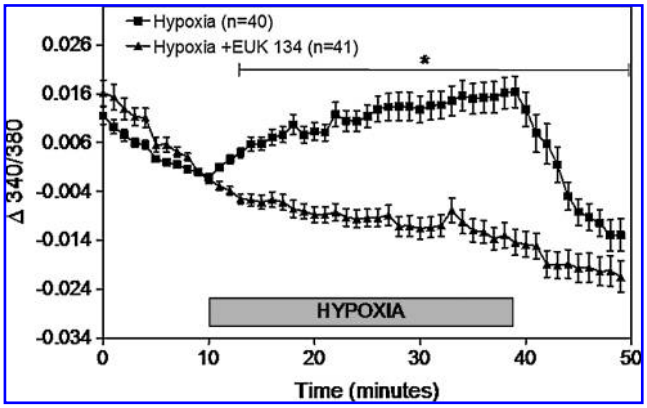

FIG. 7. Calcium-mediated changes in FURA-2 340/380 ratio measured in cells within the wall of pulmonary arteries in lung slices. The hypoxia-induced increase in cytosolic calcium during 30 min of hypoxic superfusion was abolished by EUK134, a synthetic SOD-catalase mimetic. Values are expressed as mean ± SEM. $^*p \leq 0.05$.

reaching ~17% oxidation within 5 min after the start of hypoxia. Overexpression of cytosolic catalase significantly attenuated the hypoxia-induced oxidation of the RoGFP protein. These results indicate that the principal oxidant species mediating the RoGFP response in the cytosol must have been hydrogen peroxide.

Hypoxia elicits a rapid constriction of pulmonary arteries, which is mediated by an increase in $[Ca^{2+}]_i$. We measured hypoxia-induced intracellular calcium changes in extraluminal regions of pulmonary arteries in lung slices by using FURA-2. Superfusion of the lung slices with hypoxic media (30 min; 1.5% O_2) caused an increase in $[Ca^{2+}]_i$ demonstrated by a maximum change in the FURA-2 ratio (Δ340/380 ratio) of 0.016 ± 0.003 from normoxic levels (Fig. 6). Catalase overexpression in the lung slices significantly attenuated the $[Ca^{2+}]_i$ response to hypoxia. However, despite the overexpression of catalase, some evidence of calcium activation was still apparent. To test further the requirement for ROS signaling in triggering the increased $[Ca^{2+}]_i$ during hypoxia, lung slices were treated with the antioxidant compound EUK-134, which mimics the activity of both SOD and catalase. In the presence of EUK-134, hypoxia-induced increases in $[Ca^{2+}]_i$ were completely abolished (Fig. 7). Collectively, these findings indicate that the hypoxia-induced increase in $[Ca^{2+}]_i$ in pulmonary arteries of PCLSs requires an increase in ROS signaling.

To determine whether entry of extracellular calcium contributes to the increase in $[Ca^{2+}]_i$ elicited by hypoxia, FURA-2–loaded lung-slice responses were compared in the presence and absence of calcium in the perfusate (Fig. 8). During hypoxia, pulmonary arterial cells in lung slices demonstrated significant increases in $[Ca^{2+}]_i$ when perfused with Ca^{2+}-containing media, but no change in FURA-2 ratio was detected when slices were perfused with calcium-free media

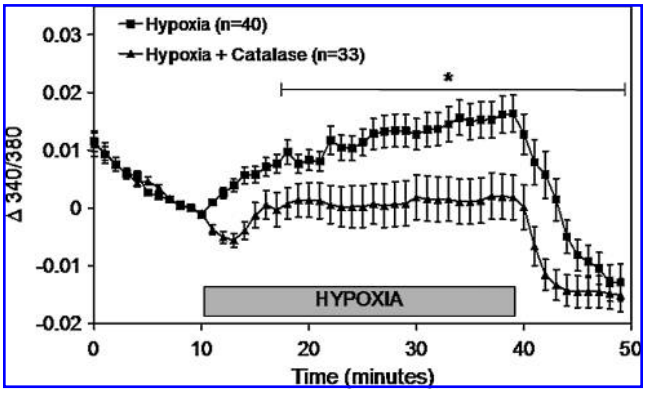

FIG. 6. Calcium-mediated changes in FURA-2 340/380 ratio measured in cells within the wall of pulmonary arteries in lung slices. The hypoxia-induced increase in cytosolic calcium during 30 min of hypoxic superfusion was attenuated in cells overexpressing catalase. Values are expressed as mean ± SEM. $^*p < 0.05$.

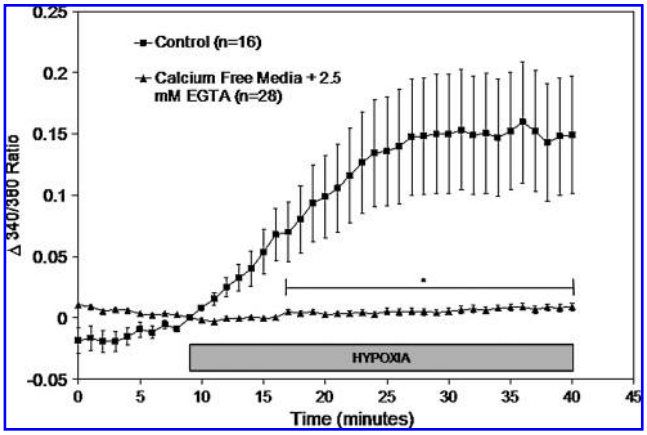

FIG. 8. Calcium-mediated changes in FURA-2 340/380 ratio within pulmonary artery cells superfused with normoxic or hypoxic (1.5% O_2) media. Superfusion with Ca^{2+}-free media containing EGTA (2.5 m*M*) abolished the hypoxia-induced increase in cytosolic ionized calcium. Values are expressed as mean ± SEM. $^*p \leq 0.05$.

containing EGTA (2.5 m*M*). Thus, entry of extracellular Ca^{2+} is the principal mechanism contributing to the increase in cytosolic calcium during hypoxia.

Discussion

The present study builds on prior work by demonstrating that acute hypoxia increases cytosolic oxidant signaling in precapillary pulmonary arterial cells within mouse lung slices. These ROS signals are then required to trigger increases in $[Ca^{2+}]_i$. To avoid the uncertainty associated with conventional oxidant probes, we assessed redox signaling with RoGFP, which was highly reduced in the cytosol under normoxic conditions. During hypoxia, we observed a subtle but significant shift toward a more oxidized state in PASMCs. This increase in oxidant signaling was significantly attenuated by overexpression of catalase, implicating increased superoxide and H_2O_2 in the response. The relation between oxidant signaling and the increase in $[Ca^{2+}]_i$ was explored by using FURA-2–labeled vascular cells, which demonstrated a significant increase in $[Ca^{2+}]_i$ during acute hypoxia. The hypoxia-induced $[Ca^{2+}]_i$ response was attenuated by overexpression of catalase and abolished by EUK-134, indicating that an oxidant signal is required for the intracellular increase in calcium and subsequent pulmonary vasoconstriction. Removal of extracellular calcium ions completely abolished the hypoxia-induced increase in $[Ca^{2+}]_i$, indicating that extracellular calcium entry is required for the HPV response. These findings support the hypothesis that hypoxia-induced increases in ROS signaling are required for the entry of extracellular $[Ca^{2+}]_i$ and subsequent contraction of pulmonary arteries during acute hypoxia.

PASMCs of intact mouse lung slices

It has been argued that cultured PASMCs can undergo phenotypic changes that may have an effect on oxidant signaling. Moreover, within the intact pulmonary artery, PASMCs may be influenced by the microenvironment and by interactions with the endothelium during acute hypoxia, thereby affecting its response through cell–cell interactions (9). To address this, we studied hypoxia-induced ROS signaling and cytosolic calcium changes in the intact arterioles of lung slices. Small intraparenchymal arteries were distinguishable from airways and venules under fluorescence microscopy because the Cell Tracker Red infusion labeled the vascular endothelial cells in the distal arterioles. Vasconstrictive properties were maintained in the microvasculature of PCLSs, as demonstrated by reduction in luminal surface area under hypoxic conditions. Although the oxidant response was sustained, a progressive loss in the calcium response evolved over 48 h in culture, indicating that phenotypic changes can still occur despite the intact microstructure.

Cytosolic oxidant-signaling changes were measured by using RoGFP, whose ratiometric behavior allows assessment of thiol redox status independent of the level of protein expression in the cells (14). Moreover, the reversible redox behavior of this sensor allows calibration of the ratios by administration of oxidizing and reducing agents at the end of the experiment, which permits calculation of the percentage of oxidation. Expression of RoGFP in the PASMCs of intact lung slices was confirmed by the colocalization of RoGFP and smooth muscle–specific desmin antibody, as observed under confocal fluorescence microscopy. To study the effects of antioxidants on cytosolic oxidant signaling, catalase was expressed in lung slices by using an adenoviral vector. Overexpression of catalase in the vascular cells was confirmed by fluorescence microscopy when compared with endogenous levels of catalase. The ability to transduce pulmonary arterioles (50–100 μm) of the lung slices with RoGFP and catalase-expressing vectors make this model useful for studying cell-specific oxidant signaling and $[Ca^{2+}]_i$ changes in response to acute hypoxia.

Increased ROS signaling triggers HPV

Our results do not support the model advocated by Michelakis, Archer, and Weir, in which hypoxia decreases the generation of ROS in PASMCs and shifts the cytosol to a more-reduced state (1, 3, 4, 10, 12, 22). They argued that a reductive stress during hypoxia alters redox-sensitive thiol groups in regulatory subunits of voltage-dependent potassium (K_v) channels, causing the channels to close. The decrease in K^+ current triggers membrane depolarization, causing voltage-gated (L-type) calcium channels to open. This leads to an influx of extracellular calcium followed by a vascular contraction. Their studies are based largely on the use of lucigenin or luminol chemiluminescence to detect ROS levels in pulmonary vessels or intact lungs (1, 2, 10, 11). However, autoxidation and limited intracellular access may interfere with the ability of lucigenin or luminol to detect intracellular oxidants. More important, these probes do not exhibit ratiometric behavior and are therefore affected by changes in concentration or path length, raising concerns about their ability to detect changes in cytosolic ROS signaling.

ROS signaling and increases in $[Ca^{2+}]_i$

We detected significant increases in $[Ca^{2+}]_i$ in pulmonary arteries during acute hypoxia, by using FURA-2. This response was attenuated by overexpression of catalase, indicating that ROS signaling, most likely involving superoxide and H_2O_2, is required for the response. Interestingly, although the RoGFP oxidation was largely abolished by catalase overexpression, catalase only blunted the $[Ca^{2+}]_i$ response, yet EUK-134, which scavenges both H_2O_2 and superoxide, completely abolished it. These findings suggest that superoxide may contribute to the hypoxia-induced increase in $[Ca^{2+}]_i$ in addition to H_2O_2.

The cytosolic calcium response to hypoxia was abolished in the absence of extracellular calcium, indicating that increases in ROS signaling are required for the entry of extracellular Ca^{2+}. Although these measurements do not identify the specific calcium channels involved in the hypoxic response, recent studies by Sylvester and colleagues (17) suggest that calcium entry through store-activated calcium channels is involved in HPV.

We conclude that the hypoxia-induced increase in $[Ca^{2+}]_i$ is mediated by an increase in ROS signaling, and that redox responses to hypoxia in intact lung slices recapitulate previous studies showing hypoxia-induced increases in ROS-dependent calcium signaling in cultured PASMCs. Collectively, these observations provide evidence supporting our model of hypoxia-induced oxidant signaling mediating the increase in $[Ca^{2+}]_i$ in pulmonary arteries during HPV (21).

Acknowledgments

We thank Danijela Dokic for her technical assistance. This study was supported by NIH grants HL35440, and HL079650, and HL66315 (P.T.S.), NS056313 (J.D.M.), and HL086715 (K.N.F.).

References

1. Archer SL, Huang J, Henry T, Peterson D, and Weir EK. A redox-based O_2 sensor in rat pulmonary vasculature. *Circ Res* 73: 1100–1112, 1993.
2. Archer SL, Peterson D, Nelson DP, DeMaster EG, Kelly B, Eaton JW, and Weir EK. Oxygen radicals and antioxidant enzymes alter pulmonary vascular reactivity in the rat lung. *J Appl Physiol* 66: 102–111, 1989.
3. Archer SL, Souil E, Dinh-Xuan AT, Schremmer B, Mercier JC, El Yaagoubi A, Nguyen-Huu L, Reeve HL, and Hampl V. Molecular identification of the role of voltage-gated K^+ channels, Kv1.5 and Kv2.1, in hypoxic pulmonary vasoconstriction and control of resting membrane potential in rat pulmonary artery myocytes. *J Clin Invest* 101: 2319–2330, 1998.
4. Archer SL, Weir EK, Reeve HL, and Michelakis E. Molecular identification of O_2 sensors and O_2-sensitive potassium channels in the pulmonary circulation. *Adv Exp Med Biol* 475: 219–240, 2000.
5. Dooley CT, Dore TM, Hanson GT, Jackson WC, Remington SJ, and Tsien RY. Imaging dynamic redox changes in mammalian cells with green fluorescent protein indicators. *J Biol Chem* 279: 22284–22293, 2004.
6. Gutscher M, Pauleau AL, Marty L, Brach T, Wabnitz GH, Samstag Y, Meyer AJ, and Dick TP. Real-time imaging of the intracellular glutathione redox potential. *Nat Methods* 5: 553–559, 2008.
7. Hanson GT, Aggeler R, Oglesbee D, Cannon M, Capaldi RA, Tsien RY, and Remington SJ. Investigating mitochondrial redox potential with redox-sensitive green fluorescent protein indicators. *J Biol Chem* 279: 13044–13053, 2004.
8. Liu JQ, Sham JS, Shimoda LA, Kuppusamy P, and Sylvester JT. Hypoxic constriction and reactive oxygen species in porcine distal pulmonary arteries. *Am J Physiol Lung Cell Mol Physiol* 285: 322–333, 2003.
9. Liu Q, Sham JSK, Shimoda LA, and Sylvester JT. Hypoxic constriction of porcine distal pulmonary arteries: endothelium and endothelin dependence. *Am J Physiol Lung Cell Mol Physiol* 280: L856–L865, 2001.
10. Michelakis ED, Hampl V, Nsair A, Wu XC, Harry G, Haromy A, Gurtu R, and Archer SL. Diversity in mitochondrial function explains differences in vascular oxygen sensing. *Circ Res* 90: 1307–1315, 2002.
11. Mohazzab KM and Wolin MS. Properties of a superoxide anion-generating microsomal NADH oxidoreductase, a potential pulmonary artery Po_2 sensor. *Am J Physiol* 267: L823–L831, 1994.
12. Moudgil R, Michelakis ED, and Archer SL. Hypoxic pulmonary vasoconstriction. *J Appl Physiol* 98: 390–403, 2005.
13. Paddenberg R, Konig P, Faulhammer P, Goldenberg A, Pfeil U, and Kummer W. Hypoxic vasoconstriction of partial muscular intra-acinar pulmonary arteries in murine precision cut lung slices. *Respir Res* 7: 93, 2006.
14. Remington SJ. Fluorescent proteins: maturation, photochemistry and photophysics. *Curr Opin Struct Biol* 16: 714–721, 2006.
15. Wallenstein S, Zucker CL, and Fleiss JL. Some statistical methods useful in circulation research. *Circ Res* 47: 1–9, 1980.
16. Wang J, Shimoda LA, and Sylvester JT. Capacitative calcium entry and TRPC channel proteins are expressed in rat distal pulmonary arterial smooth muscle. *Am J Physiol Lung Cell Mol Physiol* 286: L848–L858, 2004.
17. Wang J, Shimoda LA, Weigand L, Wang WQ, Sun DJ, and Sylvester JT. Acute hypoxia increases intracellular $[Ca^{2+}]$ in pulmonary arterial smooth muscle by enhancing capacitative Ca^{2+} entry. *Am J Physiol Lung Cell Mol Physiol* 288: L1059–L1069, 2005.
18. Waypa GB, Chandel NS, and Schumacker PT. Model for hypoxic pulmonary vasoconstriction involving mitochondrial oxygen sensing. *Circ Res* 88: 1259–1266, 2001.
19. Waypa GB, Guzy R, Mungai PT, Mack MM, Marks JD, Roe MW, and Schumacker PT. Increases in mitochondrial reactive oxygen species trigger hypoxia-induced calcium responses in pulmonary artery smooth muscle cells. *Circ Res* 99: 970–978, 2006.
20. Waypa GB, Marks JD, Mack MM, Boriboun C, Mungai PT, and Schumacker PT. Mitochondrial reactive oxygen species trigger calcium increases during hypoxia in pulmonary arterial myocytes. *Circ Res* 91: 719–726, 2002.
21. Waypa GB and Schumacker PT. Hypoxic pulmonary vasoconstriction: redox events in oxygen sensing. *J Appl Physiol* 98: 404–414, 2005.
22. Weir EK and Archer SL. The mechanism of acute hypoxic pulmonary vasoconstriction: a tale of two channels. *FASEB J* 9: 183–189, 1995.
23. Weir EK, Lopez-Barneo J, Buckler KJ, and Archer SL. Mechanisms of disease: acute oxygen-sensing mechanisms. *N Engl J Med* 353: 2042–2055, 2005.

Address correspondence to:
Paul T. Schumacker, Ph.D.
Department of Pediatrics
Northwestern University
Ward Building 12-191
303 East Chicago Avenue
Chicago, IL 60611

E-mail: p-schumacker@northwestern.edu

Date of first submission to ARS Central, August 31, 2009; date of acceptance, September 11, 2009.

Abbreviations Used

ANOVA = analysis of variance
PA = pulmonary artery
PAECs = pulmonary artery endothelial cells
PASMCs = pulmonary artery smooth muscle cells
ROS = reactive oxygen species

This article has been cited by:

1. Yanlong Liu, Chunhong Wang, Yuhua Wang, Zhenhua Ma, Jian Xiao, Craig McClain, Xiaokun Li, Wenke Feng. 2012. Cobalt chloride decreases fibroblast growth factor-21 expression dependent on oxidative stress but not hypoxia-inducible factor in Caco-2 cells. *Toxicology and Applied Pharmacology* **264**:2, 212-221. [CrossRef]
2. Alicia Izquierdo-Álvarez, Elena Ramos, Joan Villanueva, Pablo Hernansanz-Agustín, Rubén Fernández-Rodríguez, Daniel Tello, Montserrat Carrascal, Antonio Martínez-Ruiz. 2012. Differential redox proteomics allows identification of proteins reversibly oxidized at cysteine residues in endothelial cells in response to acute hypoxia. *Journal of Proteomics* **75**:17, 5449-5462. [CrossRef]
3. Jiwei Zhang , Juan Zhou , Lei Cai , Yankai Lu , Tao Wang , Liping Zhu , Qinghua Hu . 2012. Extracellular Calcium-Sensing Receptor Is Critical in Hypoxic Pulmonary Vasoconstriction. *Antioxidants & Redox Signaling* **17**:3, 471-484. [Abstract] [Full Text HTML] [Full Text PDF] [Full Text PDF with Links] [Supplemental material]
4. A.-B. Al-Mehdi, V. M. Pastukh, B. M. Swiger, D. J. Reed, M. R. Patel, G. C. Bardwell, V. V. Pastukh, M. F. Alexeyev, M. N. Gillespie. 2012. Perinuclear Mitochondrial Clustering Creates an Oxidant-Rich Nuclear Domain Required for Hypoxia-Induced Transcription. *Science Signaling* **5**:231, ra47-ra47. [CrossRef]
5. Su Jung Park, Hae Young Yoo, Hye Jin Kim, Jin Kyoung Kim, Yin-Hua Zhang, Sung Joon Kim. 2012. Requirement of Pretone by Thromboxane A 2 for Hypoxic Pulmonary Vasoconstriction in Precision-cut Lung Slices of Rat. *The Korean Journal of Physiology & Pharmacology* **16**:1, 59. [CrossRef]
6. Stephen Wedgwood, Paul T. Schumacker, Robin H. SteinhornHypoxia and Hyperoxia 91-109. [CrossRef]
7. O. F. Araneda, M. Tuesta. 2012. Lung Oxidative Damage by Hypoxia. *Oxidative Medicine and Cellular Longevity* **2012**, 1-18. [CrossRef]
8. Manish Mittal, Xiang Q. Gu, Oleg Pak, Matthew E. Pamenter, Daniela Haag, D. Beate Fuchs, Ralph T. Schermuly, H.A. Ghofrani, Ralf P. Brandes, Werner Seeger, Friedrich Grimminger, Gabriel G. Haddad, Norbert Weissmann. 2011. Hypoxia induces Kv channel current inhibition by increased NADPH oxidase-derived reactive oxygen species. *Free Radical Biology and Medicine* . [CrossRef]
9. L. Boardman, J. S. Terblanche, S. K. Hetz, E. Marais, S. L. Chown. 2011. Reactive oxygen species production and discontinuous gas exchange in insects. *Proceedings of the Royal Society B: Biological Sciences* . [CrossRef]
10. Priti Azad, Julie Ryu, Gabriel G. Haddad. 2011. Distinct role of Hsp70 in Drosophila hemocytes during severe hypoxia. *Free Radical Biology and Medicine* **51**:2, 530-538. [CrossRef]
11. Michael J. Sanderson. 2011. Exploring lung physiology in health and disease with lung slices. *Pulmonary Pharmacology & Therapeutics* . [CrossRef]
12. Frank Funke, Florian J. Gerich, Michael Müller. 2011. Dynamic, semi-quantitative imaging of intracellular ROS levels and redox status in rat hippocampal neurons. *NeuroImage* **54**:4, 2590-2602. [CrossRef]
13. Michelle J. Connolly, Philip I. Aaronson. 2010. Cell redox state and hypoxic pulmonary vasoconstriction: Recent evidence and possible mechanisms#. *Respiratory Physiology & Neurobiology* **174**:3, 165-174. [CrossRef]
14. Nanduri R. Prabhakar, Ganesh K. Kumar, Jayasri Nanduri. 2010. Intermittent hypoxia augments acute hypoxic sensing via HIF-mediated ROS#. *Respiratory Physiology & Neurobiology* **174**:3, 230-234. [CrossRef]
15. E. Kenneth Weir, Stephen L. Archer. 2010. The role of redox changes in oxygen sensing#. *Respiratory Physiology & Neurobiology* **174**:3, 182-191. [CrossRef]
16. Gregory B. Waypa, Paul T. Schumacker. 2010. Hypoxia-induced changes in pulmonary and systemic vascular resistance: Where is the O2 sensor?#. *Respiratory Physiology & Neurobiology* **174**:3, 201-211. [CrossRef]
17. Andreas J. Meyer , Tobias P. Dick . 2010. Fluorescent Protein-Based Redox Probes. *Antioxidants & Redox Signaling* **13**:5, 621-650. [Abstract] [Full Text HTML] [Full Text PDF] [Full Text PDF with Links]
18. David Jourd'heuil . 2010. Redox Control of Vascular Smooth Muscle Function. *Antioxidants & Redox Signaling* **12**:5, 579-581. [Citation] [Full Text HTML] [Full Text PDF] [Full Text PDF with Links]